Journal of Physics: Conference Series

PAPER • **OPEN ACCESS**

Computational fluid dynamic modelling of supersonic ejectors: comparison between 2D and 3D modelling

To cite this article: Giorgio Besagni *et al* 2021 *J. Phys.: Conf. Ser.* **2116** 012091

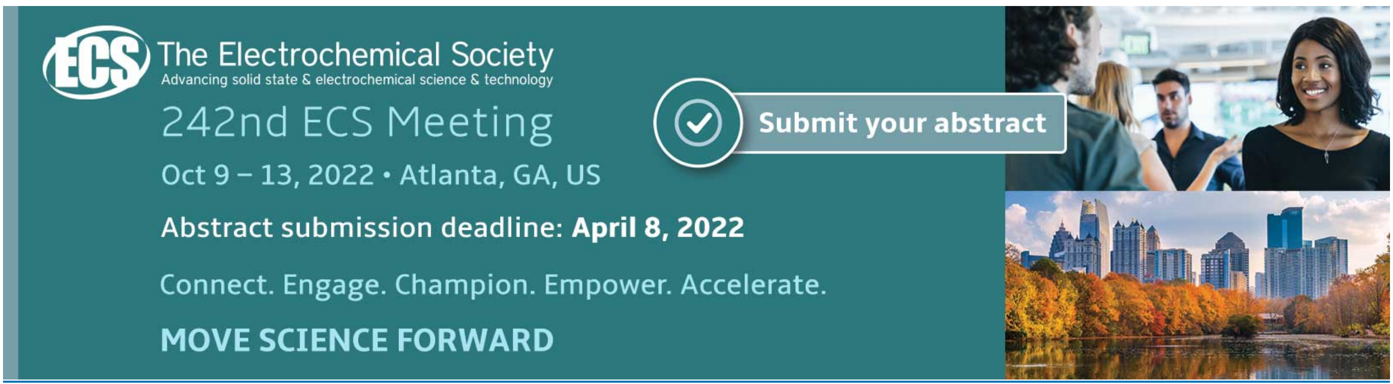

Computational fluid dynamic modelling of supersonic ejectors: comparison between 2D and 3D modelling

Giorgio Besagni[1], Lorenzo Croci[1], Nicolò Cristiani[1,2], Fabio Inzoli[2] and Gaël Raymond Guédon[2]

[1]Ricerca sul Sistema Energetico - RSE S.p.A., Power System Development Department, via Rubattino 54, 20134 Milano (Italy)
[2] Politecnico di Milano, Department of Energy, via Lambruschini 4a, 20156, Milano (Italy)

giorgio.besagni@polimi.it

Abstract. It is known that the global performances of ejector-based systems (viz., at the "*global-scale*") depend on the local flow properties within the ejector (viz., at the "*local-scale*"). For this reason, reliable computational fluid-dynamics (*CFD*) approaches, to obtain a precise and an a-priori knowledge of the local flow phenomena, are of fundamental importance to support the deployment of innovative ejector-based systems. This communication contributes to the existing discussion by presenting a numerical study of the turbulent compressible flow in a supersonic ejector. In particular, this communication focuses on a precise knowledge gap: the comparison between *2D* and *3D* modelling approaches as well as density-based and pressure-based solvers. The different approaches have been compared and validated against literature data consisting in entrainment ratio and wall static pressure measurements. In conclusion, this paper is intended to provide guidelines for researchers dealing with the numerical simulation of ejectors.

1. Introduction

Ejector is a flow device that provides a combined effect of compression, mixing and entrainment, with no-moving parts and without limitations concerning working fluids. As the performances of ejector-based systems depend on the local flow properties, reliable computational fluid-dynamics (*CFD*) approaches, to obtain a precise and an a-priori knowledge of the local flow phenomena, are of fundamental importance to support the development of innovative ejector-based systems. This communication focuses on a precise knowledge gap: the comparison between *2D* and *3D* modelling approaches as well as density-based and pressure-based solvers. Based on the previous literature, an agreement on the influence of the *2D*/*3D* geometrical discretization and the solver selection is not reached. As for the geometrical discretization, Śmierciew et al. [1] and Sharifi and Boroomand [2] stated that *3D* simulations do not allow significant improvements compared with *2D* axial-symmetric simulations. Mazzelli et al. [3] stated that a *3D* approach may be beneficial: the wall effect associated with the front and back walls of the test section induces a significant loss due to friction that cannot be captured by a *2D* approach. As for the solver, although density-based solvers are traditionally preferred for supersonic flows involving shock waves, pressure-based algorithms (with coupled pressure-velocity coupling) have been successfully tested on ejectors, showing promising performances. Van Vu N and Kracik [4] stated that a pressure-based solver provides results quite similar to a density-based solved; however, the former showed more stable simulations and faster convergence. The same conclusion was observed by Croquer [5]. A summary of all above-mentioned papers is proposed in Table 1. This communication contributes to the present day discussion, by comparing *2D* and *3D* modelling approaches as well as density-based and pressure-based solvers. In particular, the well-known benchmark of Sriveerakul et al. [6] is used.

Table 1. Literature survey.

Reference	Solver	Mesh details	Turbulence modelling
[1]	Pressure-based	67,923 (2D) 3,520.926 (3D)	*k-ωSST*
[2]	Density-based	35,600 (2D) 721,600 (3D)	*k-ε RNG*
[3]	Density-based	75,000 (2D) 750,000 (3D)	*k-ε*, *k-ε Realizable*, *k-ωSST*, *RSM*
[4]	Density-based Pressure-based	266,000 (2D)	*k-ωSST*
[5]	Pressure-based	645,000 (2D)	*k-ε*, *k-ε Realizable*, *k-ωSST*, *RNG*

2. Methods: benchmark and numerical modelling

2.1. Benchmark

The validation of the numerical model has been ensured by using the experimental dataset provided by Sriveerakul et al. [6]. In this study, both global (ω the entrainment ratio; viz., the ratio between the secondary and the primary mass flow rate) and local (wall static pressure along the ejector) measurements are available for a complete validation of the approach. The boundary conditions for the tested case are presented in Figure 1; The entrainment ratio for the tested case is equal to ω_{exp} = 0.309.

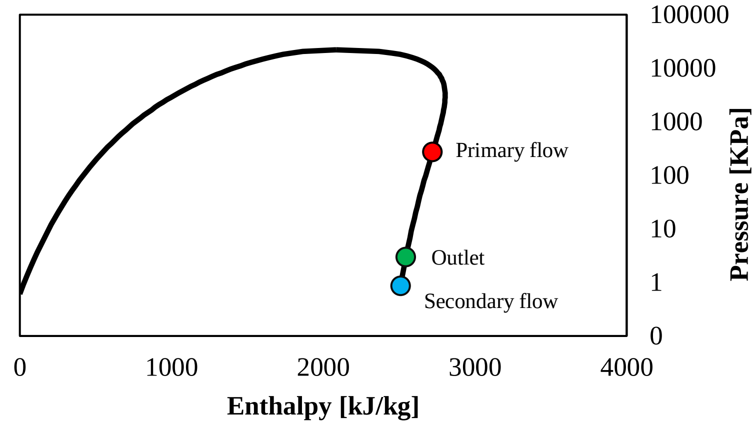

Figure 1. Boundary conditions for the tested case. Primary flow: 130 °C, 270280 Pa; Secondary flow: 5 °C, 872.5 Pa; Outlet: 24.08 °C, 3000 Pa.

2.2. Numerical modelling

The finite volume commercial code ANSYS Fluent (*Release 19 - R3*) has been used to solve the steady state Reynolds Averaged Navier-Stokes (*RANS*) equations for the turbulent compressible Newtonian fluid flow, employing the *k-ω SST* model, which was found the most suitable turbulence model by Besagni and Inzoli [7]. Turbulence boundary conditions are implemented as follows: hydraulic diameter and the turbulent intensity (5% for the primary flows and 2% for the secondary one), as described [7]. Second order upwind numerical schemes have been used for the spatial discretization, in order to limit the numerical diffusion. Second order upwind schemes also for the turbulence model variables have been used. Gradients are evaluated by a least-squares approach. The initialization has been performed by a two-step approach: (i) an hybrid initialization followed by a (ii) full multi-grid (*FMG*) scheme. The numerical solution is considered as converged when the normalized difference of mass flow rates at the inlets and at outlet is less than 10^{-5} and the mass flow-rate variation of primary and secondary flow on the last 50 iteration is less than 10^{-5}. As mentioned above, both pressure-based and density-based solvers are tested and compared. As for the geometrical modeling, both *2D* (axialsymmetric) and *3D* geometrical discretization are tested. The *2D*-axial symmetric structured mesh is built as follows: (i) maximum aspect ratio of 3; (ii) a wall refinement is adopted to ensure $y^+ = 1$; (iii) during simulations two cycles of refinement, based on Mach gradient criteria (Mach gradient scaled on global maximum more than 0.1), are used. The *3D* poliedric mesh is built as follows: (i) the boundary layer consists of 15 layers; (ii) during simulations a cycle of refinement, based on Mach gradient criteria (Mach gradient scaled based on global maximum more than 0.1), is used. The details and the code names of the tested cases are presented in Table 2.

Table 2. Details of the tested cases.

Code Name	Solver details	Final mesh size
$2D_d$	Density-based	526,752
$3D_d$	Density-based	3,524,080
$2D_p$	Pressure-based	434,517
$3D_p$	Pressure-based	5,008,675

3. Results

Herein, the results are presented and discussed in terms of the global and the local flow properties. In particular, Figure 2 displays the wall profiles and Figure 3 displays the Mach contours. In addition, Table 3 displays the numerical entrainment ratios, the relative error of the entrainment ratios (Eq. 1) and the mean absolute error of the wall pressure profiles (Eq. 2), defined as follows:

$$\text{Relative error} = \frac{\omega_{CFD} - \omega_{EXP}}{\omega_{EXP}} \tag{1}$$

$$\text{Mean absolute error} = \sum \frac{|p_{CFD} - p_{EXP}|}{p_{EXP}} \tag{2}$$

Table 3. Results for the tested cases (ω_{Exp} = 0.309).

Code Name	ω_{CFD}	Relative error, Eq. (1) [%]	Mean absolute error, Eq. (2) [%]
$2D_d$	0.307	-0.77%	9.28%
$3D_d$	0.310	0.22%	10.06%
$2D_p$	0.314	1.73%	9.45%
$3D_p$	0.316	2.25%	9.55%

All tested cases are able to predict the global and the local flow properties. As for the solvers, on the global point of view, the entrainment ratios for pressure-based solver, for both *2D* and *3D* cases, are slightly higher compared with the ones predicted by density-based solver. On the local point of view, both solvers provide good agreements with the local wall pressure profile. As for the geometrical modeling, the entrainment ratios predicted by the *3D* approach are similar to the *2D* ones. Conversely, on the local point of view, the pressure-based solver seems to predict higher wall pressure oscillations compared with the density-based solver. In general, both the pressure-based and the density-based solvers are able to correctly predict the ejector fluid dynamics and using a *3D* approach does not improve the predictive capability. Looking at the Mach contours (Figure 3), it is noted that the under-expanded wave at the nozzle exit is well described by all the tested cases. Some differences are observed for the *2D* cases, when describing the second shock train before the diffuser. The pressure-based predicts an oblique shock waves at the entrance of the diffuser, whereas the density-based solver predicts a smoother pressure recovery. This feature is less marked within the *3D* cases.

4. Conclusions

Based on the global and the local outcomes of this study, it is concluded that there are no significant improvement when using a *3D* approach compared with a 2D axial-symmetric approach, in agreement with refs [1,2]. In addition, both pressure-based and density-based solver are suitable to predict ejector fluid dynamics, however, it should be noted that the former exhibites faster convergence.

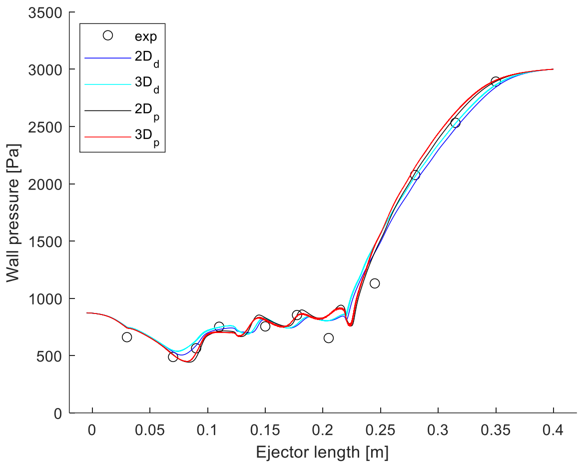

Figure 2. Wall pressure profiles: comparison between the different cases.

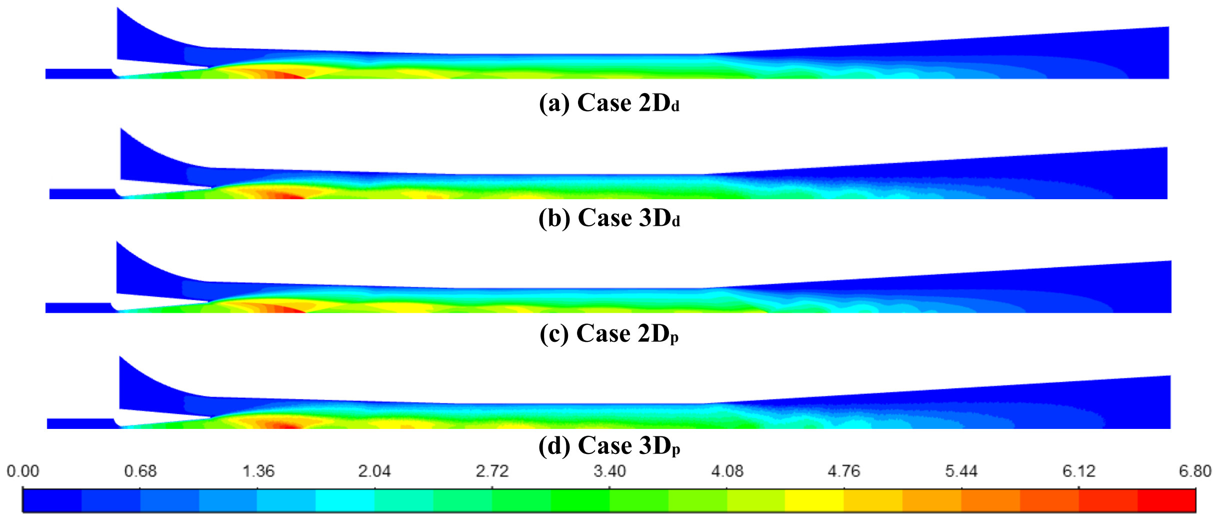

Figure 3. Mach contours: comparison between the different cases.

Acknowledgements

This work has been financed by the Research Fund for the Italian Electrical System in compliance with the Decree of Minister of Economic Development April 16, 2018.

References

[1] Smierciew K Gagan J and Butrymowicz D 2019 *Appl Therm Eng* **149** 85-93
[2] Sharifi N and Boroomand M 2013 *Energy Convs Manage* **69** 217-27
[3] Mazzelli F Little AB Garimella S and Bartosiewicz Y 2015 *Int. J. Heat Fluid Fl* **56** 305-16
[4] Van Vu N and Kracik J 2018 *EPJ Web of Conferences* **180**, 02075 (2018)
[5] Croquer S 2018 *Combined PhD Thesis Université de Sherbrooke Faculté de genie Département de génie mécanique*
[6] Sriveerakul T Aphornratana S and Chunnanond K 2007 *Int J Therm Sci* **46** 812-22
[7] Besagni G and Inzoli F 2017 *Appl Therm Eng.* **117** 122-44